

Quantum limits for the precision of optical parameter estimation of arbitrarily shaped phase objects

Arturo Villegas,¹ M. H. M. Passos,¹ and Juan P. Torres^{1,2}

¹*ICFO—Institut de Ciències Fotoniques, the Barcelona Institute of Science and Technology, 08860 Castelldefels (Barcelona), Spain*^{*}

²*Department of Signal Theory and Communications,
Universitat Politècnica de Catalunya, 08034 Barcelona, Spain*

(Dated: March 1, 2023)

Using tools from quantum estimation theory, we derive precision bounds for the estimation of parameters that characterize phase objects. We compute the Crámer-Rao lower bound for two experimentally relevant types of multimode quantum states: N copies of a single-photon state and a coherent state with mean photon number N . We show that the equivalence between them depends on the symmetry of the phase. We apply these results to estimate the dispersion parameters of an optical fiber as well as the height and sidewall angle of a cliff-like nanostructure, relevant for semiconductor circuits.

Introduction. — Phase objects are samples that modify the phase, but not the amplitude of a probe light wave after being transmitted/reflected from them. Although this is true in the near field, non-uniform phase changes might lead as well to changes in the amplitude of the outgoing light wave in the far field. As examples of phase objects, one can think of biological samples that are mostly transparent at visible and infrared frequency bands, and whose longitudinal thickness changes along the transverse dimensions [1], a highly reflective surface such as a 1D-periodic diffraction grating [2, 3], or a highly dispersive optical fiber.

To characterize the object, one can consider two different approaches. In an imaging scenario, one aims at retrieving a full image of the sample with the best transverse spatial resolution available. In a parameter estimation scenario, the interest is to estimate a set of parameters with good accuracy and precision; which requires the use of unbiased estimators [4]. Assuming that this is the case, the precision available in an experiment will ultimately determine our ability to retrieve the true values of the set of parameters with a small error [5].

One central question is thus to determine what precision is available for different experimental schemes. The classical Cramér-Rao (CR) bound sets a precision bound determined by the set of possible results that can be obtained using a specific measurement technique. Since this bound depends on the use of a specific detection scheme, one can always wonder if a different detection scheme could provide a more precise estimation.

The quantum Cramér-Rao (QCR) bound [4, 6] solves this issue by setting a fundamental precision bound that is independent of any specific measurement scheme considered. Its value depends only on the type of light wave that illuminates the object, i.e., the quantum state, and

the nature of the light-matter interaction that modifies the characteristics of the input light beam. The latter depends on the parameters to be estimated and its study allows to retrieve their values. The QCR bound is used nowadays in many different scenarios to establish fundamental precision limits [7–10], and has replaced at the fundamental level former sensitivity limits obtained using alternative methods [11].

The QCR bound is obtained by means of the quantum Fisher information matrix (QFIM). The difficulty of its calculation depends of the nature of the quantum state considered, as well as the number of parameters of interest (*single- or multiparameter quantum estimation*). For different cases, techniques and expressions have been developed to calculate the QFIM, and thus the QCR bound [6, 12–18].

An important consideration is to determine the most informative precision bound, i.e., a bound that can be reached ideally by a certain measurement scheme, although the scheme might be unknown or difficult to implement experimentally. For the case of single parameter estimation, the QCR bound, given by the inverse of the QFIM is the most informative bound [13]. However, for multiparameter estimation this is not the case in general. In this work we demonstrate that for the estimation of phases introduced by phase objects the QCR bound is the most informative even for the estimation of multiple parameters. We highlight the relevance of this result for optical metrology of phase objects.

In some cases of interest the theoretical analysis of the QFIM is made considering that the source of light consists of N copies of a single-photon multimode quantum state, even though the light source does not actually generate single-photon quantum states. For instance, in Ref. [9] they justify using single-photon states for analysing weak thermal sources at optical frequencies by claiming that the source is “*effectively emitting at most one photon*”, and that “*it allows us to describe the quantum state*

* arturo.villegas@icfo.eu

ρ of the optical field on the image plane as a mixture of a zero-photon state ρ_0 and a one-photon state ρ_1 in each time interval". One is thus assuming that "...the probability of more than one photon arriving at the image plane is negligible", as stated in Ref. [19].

In some other experiments, the theoretical calculations are done assuming a light source that generates single-photon quantum states, while experiments are done using intense or attenuated laser sources [8, 20, 21]. In a sense, this analysis seems to be motivated by the fact even though the QFIM is an inherently quantum concept, whose terms are calculated with quantum mechanics tools, in certain occasions the precision bounds can also applied to experiments where the quantum nature of light is irrelevant [8].

Motivated by the previous considerations, here we obtain and compare the QFIM, and thus the associated QCR bounds, for parameter estimation of phase objects using the aforementioned types of multimode quantum states, i.e. N copies of a single-photon state and a coherent state with average photon number N . We show that the precision bounds obtained in both cases do not coincide in general, leading to conclude the nonequivalence of these two quantum states for quantum phase estimation. However, if certain symmetry conditions are satisfied, the resulting QFIM is the same in both cases and the equivalence of the quantum states is re-established. We discuss some examples that help to clarify these results.

The analysis presented here, together with the examples that we discuss, might constitute a word of caution for experiments aimed at determining the QFIM using weak coherent states while employing single-photon quantum states, for the sake of simplicity or as an approximation, in the corresponding theoretical analysis.

The quantum Fisher information matrix. – In a quantum phase estimation protocol, particularly in the case of a non-imaging scheme for metrology of phase objects, we aim at estimating a set of M parameters ($\theta \equiv \{\theta_i\}, i = 1 \dots M$) that characterize a sample. For the sake of simplicity, we consider the state of the probe beam being a pure state ($\rho(\theta) = |\Phi(\theta)\rangle\langle\Phi(\theta)|$), a situation that is experimentally relevant and conveniently simplifies the calculations. The elements F_{ij} of the QFIM are given by

$$F_{ij} = 4 \left[\langle \Phi_i | \Phi_j \rangle + \langle \Phi | \Phi_i \rangle \langle \Phi | \Phi_j \rangle \right], \quad (1)$$

where $|\Phi_i\rangle \equiv |\partial\Phi/\partial\theta_i\rangle$. For any unbiased estimator $\hat{\theta}$ of the set of parameters θ , it holds that [4]

$$[V(\hat{\theta})]_{ij} \geq [F^{-1}]_{ij}, \quad (2)$$

where V is the covariance matrix. Note that Eq. (2) has to be understood in a matrix way, i.e., the matrix $[V(\hat{\theta}) - F^{-1}]$ is positive semidefinite.

In the framework of multiparameter estimation with pure states, the QFIM provides the most informative bound if $\text{Im}\langle\Phi_i|\Phi_j\rangle = 0$ for $i, j = 1 \dots M$ [14, 17]. This condition can be easily shown to be equivalent to $\langle\Phi_i|\Phi_j\rangle = \langle\Phi_j|\Phi_i\rangle$. The calculations that we hereby present demonstrate that these conditions are fulfilled for parameter estimation of phase objects probed by the two types of quantum states consider in this work, coherent and single-photon multimode quantum states.

One word of caution might be helpful here. When considering physical scenarios that involve optical phases and interferometers, one has to be careful with the selection of the quantum state that describes the experimental scheme, since apparently equal physical models can lead to different values of the QCR bound. This might cause *interpretation problems* concerning the bounds obtained via the QFIM [22]. Considering non-uniform phases can help to avoid some of these issues, since we can use as a reference the phase at a specific spatial location, or at a specific frequency.

QFIM for N copies of a single-photon multimode quantum state. – We consider the probing light wave consisting of N independent single photons with input state $|\Phi_0\rangle = \int dx f(x)|x\rangle$. For the sake of simplicity we refer to x as spatial coordinate, although it can also be another variable, e.g. the frequency. We assume that quantum states satisfies the normalization condition $\int dx |f(x)|^2 = 1$.

After interaction with a phase object, the quantum state $|\Phi\rangle$ that describes the outgoing light wave is

$$|\Phi\rangle = \int dx f(x) \exp\left\{i\varphi(x, \theta)\right\} |x\rangle, \quad (3)$$

where $\varphi = \varphi(x, \theta)$ is the phase added to the input state.

Making use of the explicit derivatives of Eq. (3), we obtain

$$\langle\Phi|\Phi_i\rangle = \int dx |f(x)|^2 \left[\frac{\partial\varphi(x)}{\partial\theta_i} \right] \quad (4)$$

and

$$\langle\Phi_i|\Phi_j\rangle = \int dx |f(x)|^2 \left[\frac{\partial\varphi(x)}{\partial\theta_i} \right] \left[\frac{\partial\varphi(x)}{\partial\theta_j} \right]. \quad (5)$$

Note that Eq. (5) shows that $\langle\Phi_i|\Phi_j\rangle$ is real, so we can deduce that the QCR bound is the most informative precision bound.

We can write the elements of the quantum Fisher information matrix F_{ij}^s , given by Eq. (1), as

$$F_{ij}^s = 4N \left\{ \int dx |f(x)|^2 \left[\frac{\partial\varphi}{\partial\theta_i} \right] \left[\frac{\partial\varphi}{\partial\theta_j} \right] - \left[\int dx |f(x)|^2 \left(\frac{\partial\varphi}{\partial\theta_i} \right) \right] \left[\int dx |f(x)|^2 \left(\frac{\partial\varphi}{\partial\theta_j} \right) \right] \right\}. \quad (6)$$

Here, Eq. (6) corresponds to the QFIM after generating N independent copies of the quantum state.

QFIM for a coherent multimode quantum state with mean photon number N . – We consider now a coherent multimode quantum state as illumination which can be defined in terms of single-mode quantum states $|\alpha_i\rangle = D(\alpha_i)|\text{vac}\rangle = \exp(\alpha_i \hat{a}_i^\dagger - \alpha_i^* \hat{a}_i)|\text{vac}\rangle$, where $D(\alpha_i)$ is the displacement operator and the mode normalization $\langle \alpha_i | \alpha_i \rangle = 1$ holds. The coherent multimode state $|\Phi\rangle$ with $N = \sum_i |\alpha_i|^2$ mean photon number can be written as [23]

$$|\Phi\rangle = |\alpha_1\rangle \dots |\alpha_N\rangle = D(\alpha_1) \dots D(\alpha_N) |\text{vac}\rangle. \quad (7)$$

The inner products in Eq. (1) have the form

$$\langle \Phi | \Phi_i \rangle = \sum_k \langle \alpha_k | \frac{\partial \alpha_k}{\partial \theta_i} \rangle \quad (8)$$

and

$$\langle \Phi_i | \Phi_j \rangle = \sum_k \langle \frac{\partial \alpha_k}{\partial \theta_i} | \frac{\partial \alpha_k}{\partial \theta_j} \rangle + \sum_{k \neq k'} \langle \frac{\partial \alpha_k}{\partial \theta_i} | \alpha_{k'} \rangle \langle \alpha_{k'} | \frac{\partial \alpha_k}{\partial \theta_j} \rangle. \quad (9)$$

Making use of the expression for the derivative of a coherent state [24]

$$\langle \frac{\partial \alpha_k}{\partial \theta_i} | = i \alpha_k \left(\frac{\partial \varphi_k}{\partial \theta_i} \right) a_k^\dagger | \alpha_k \rangle, \quad (10)$$

the inner products become

$$\langle \frac{\partial \alpha_k}{\partial \theta_i} | \frac{\partial \alpha_k}{\partial \theta_j} \rangle = |\alpha_k|^2 \left(\frac{\partial \varphi_k}{\partial \theta_i} \right) \left(\frac{\partial \varphi_k}{\partial \theta_j} \right) (1 + |\alpha_k|^2) \quad (11)$$

and

$$\langle \alpha_k | \frac{\partial \alpha_k}{\partial \theta_i} \rangle = i |\alpha_k|^2 \left(\frac{\partial \varphi_k}{\partial \theta_i} \right). \quad (12)$$

We observe again that the inner product $\langle \Phi_i | \Phi_j \rangle$ is real for $i, j = 1, \dots, M$; which implies that the QCR bound is the most informative bound. Then, the elements F_{ij}^c of the QFIM are

$$F_{ij}^c = 4 \sum_k |\alpha_k|^2 \left(\frac{\partial \varphi_k}{\partial \theta_i} \right) \left(\frac{\partial \varphi_k}{\partial \theta_j} \right). \quad (13)$$

For the sake of comparison with the corresponding expression for a single-photon multimode quantum state in Eq. (6), we write Eq. (13) in integral form as

$$F_{ij}^c = 4N \int dx |\alpha(x)|^2 \left[\frac{\partial \varphi}{\partial \theta_i} \right] \left[\frac{\partial \varphi}{\partial \theta_j} \right], \quad (14)$$

where $\alpha(x)$ is a normalized continuous function, i.e., $\int dx |\alpha(x)|^2 = 1$. In Appendix A we show an alternative derivation of Eq. (14).

The expressions for the QFIM in Eqs. (6) and (14) are our main results. They allow to determine if a coherent multimode quantum state with mean photon number N is equivalent (or nonequivalent) to N copies of a single-photon multimode quantum state for optical phase estimation. Given the same spatial shape of the illumination beam, i.e., $f(x) \equiv \alpha(x)$, the expressions for the QFIM in both cases are equal ($F_{ij}^s = F_{ij}^c$), if $I_i = 0$ holds for all $i = 1 \dots M$, where

$$I_i = \int dx |f(x)|^2 \left[\frac{\partial \varphi}{\partial \theta_i} \right].$$

Note that this is the case if $f(x)$ is a symmetric function, while the phase $\varphi(x, \theta)$ introduced by the object is antisymmetric. This demonstrates that the equivalence, or nonequivalence, of the QFIM calculated using the two types of quantum states considered above, depends on the symmetry on the spatial (or frequency) variable x of both the illumination beam and the acquired phase. In what follows we discuss some examples to illuminate this point.

Example I: Estimation of the height and the sidewall angle of a cliff-like structure. – We consider a cliff-like nanostructure made of a highly reflective material [3, 25]. This nanostructure is highly relevant in the semiconductor industry and it is characterized by two parameters: the height h and the sidewall angle β , as shown in the sketch in Fig. 1. In typical nanostructures, the height is a fraction of the wavelength of the incident light wave, and the sidewall angle is ideally close to 90° . However, fabrication errors produce variations around the desired values [26].

For the sake of simplicity, we approximate the slope of the nanostructure as

$$S(x) = \frac{h}{2} (1 + \tanh \alpha x). \quad (15)$$

The parameters to estimate are $\theta_1 \equiv \alpha$ and $\theta_2 \equiv h$, with $\tan \beta = \alpha h / 2$. The spatial profile of the intensity of the illumination beam used for probing is assumed to be a Gaussian function

$$|f(x)|^2 = \frac{2}{(\pi \sigma^2)^{1/2}} \exp \left\{ -\frac{2x^2}{\sigma^2} \right\}. \quad (16)$$

After reflection from the cliff-like structure, the optical beam acquires a spatially-dependent phase

$$\varphi(x) = kh (1 - \tanh \alpha x). \quad (17)$$

The elements of the quantum Fisher information matrix (see Appendix B for a detailed calculation) for the two types of quantum states considered in this work are

$$F_{11}^s = F_{11}^c = 4N \left(\frac{2}{\pi \sigma^2} \right)^{1/2} \frac{\pi^2 - 6}{9} \frac{(kh)^2}{\alpha^3}, \quad (18)$$

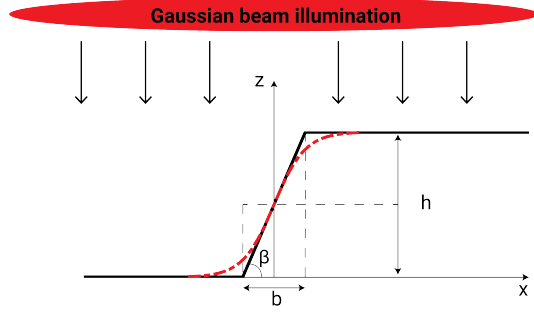


FIG. 1. Sketch of a Cliff-like nano-structure with sidewall angle β and height h . The red dashed line corresponds to the mathematical model of the slope. The sidewall angle β is related to the parameter α as $\alpha = 2/b = 2 \tan \beta/h$.

$$F_{12}^s = F_{12}^c = 4N \left(\frac{2}{\pi\sigma^2} \right)^{1/2} \frac{k^2 h}{\alpha^2}, \quad (19)$$

and

$$F_{22}^s \sim 4k^2 N, \quad F_{22}^c \sim 8k^2 N. \quad (20)$$

In order to obtain Eq. (20), we have made use of the fact that in most experimental implementations the beam waist of the Gaussian beam (σ) is much larger than the size of the cliff-like structure ($\sim 1/\alpha$), so $\alpha\sigma \gg 1$.

The QFIM is a real and symmetric 2×2 matrix. From Eq. (2), one can deduce [27] that the conditions

$$\begin{aligned} \text{Var}(\alpha) &\geq [F^{-1}]_{11} = \frac{F_{22}}{F_{11}F_{22} - [F_{12}]^2}, \\ \text{Var}(h) &\geq [F^{-1}]_{22} = \frac{F_{11}}{F_{11}F_{22} - [F_{12}]^2}. \end{aligned} \quad (21)$$

and $F_{11}F_{22} - [F_{12}]^2 \geq 0$ hold. Here $\text{Var}(y)$ designates the variance of the variable y .

For $\sigma\alpha \gg 1$ (the experimentally relevant case), we have $F_{11}F_{22} \gg [F_{12}]^2$. The relative precision error of the estimation of the parameter α is

$$\frac{\text{Var}(\alpha)}{\alpha^2} \geq \frac{9\sqrt{\pi}}{4N\sqrt{2}(\pi^2-6)} \frac{\sigma\alpha}{(kh)^2} \sim 0.72 \frac{1}{N} \frac{\sigma\alpha}{(kh)^2} \quad (22)$$

for both types of multimode quantum states. On the other hand, for the estimation of the height h , for single-photon multimode quantum states we have

$$\frac{\text{Var}(h)}{h^2} \geq \frac{1}{4N} \frac{1}{(kh)^2}, \quad (23)$$

whereas for a coherent multimode quantum state we have

$$\frac{\text{Var}(h)}{h^2} \geq \frac{1}{8N} \frac{1}{(kh)^2}. \quad (24)$$

The reason why the estimation of the parameter α with coherent and single-photon multimode quantum states gives the same result is that the derivative of the phase given by Eq. (17) with respect to the parameter α is an antisymmetric function of the spatial coordinate ($\sim x \operatorname{sech} \alpha x$) so $I_1 = 0$. This is not the case for the derivative of the phase with respect to the parameter h ($I_2 \neq 0$), hence the precision bounds given by the corresponding elements of the inverse QFIM for coherent and single-photon multimode quantum states lead to different bounds for the estimation of the height h .

Example II: Estimation of the dispersion parameters of an optical fiber. – Let us consider a pulse with a Gaussian-like shape in the angular frequency domain propagating through an optical fiber. The Gaussian spectrum of the pulse has the normalized form

$$|f(\Omega)|^2 = \frac{1}{(\pi B^2)^{1/2}} \exp\left(-\frac{\Omega^2}{B^2}\right). \quad (25)$$

Here Ω is the deviation from the central frequency and B is the bandwidth. After propagation through the fiber a distance z , the pulse acquires a frequency-dependent phase that reads

$$\varphi(\Omega) = \frac{1}{2} \beta_2 z \Omega^2 + \frac{1}{6} \beta_3 z \Omega^3, \quad (26)$$

with $\beta_{2,3}$ being the second and third order dispersion coefficients. For the sake of simplicity we ignore the presence of a global phase, and neglect any nonlinear effects of the fiber. The set of parameters to be estimated are $\theta_1 \equiv \beta_2$ and $\theta_2 \equiv \beta_3$.

It can be easily demonstrated (see further details in Appendix B) that the QFIM elements are

$$F_{22}^s = F_{22}^c = \frac{5z^2 B^6 N}{24}, \quad (27)$$

$$F_{12}^s = F_{12}^c = 0, \quad (28)$$

and

$$F_{11}^s = \frac{z^2 B^4 N}{2}, \quad F_{11}^c = \frac{3z^2 B^4 N}{4}. \quad (29)$$

The precision of the estimation of the parameter β_2 using a single-photon multimode quantum state is

$$\text{Var}(\beta_2) = \frac{2}{z^2 B^4 N} \quad (30)$$

whereas for a coherent multimode quantum state

$$\text{Var}(\beta_2) = \frac{4}{3} \frac{1}{z^2 B^4 N} \sim 0.66 \frac{2}{z^2 B^4 N}. \quad (31)$$

The precision of the estimation of the parameter β_3 , equal for both quantum states, is

$$\text{Var}(\beta_3) = \frac{24}{5} \frac{1}{z^2 B^6 N}. \quad (32)$$

The derivative of the phase with respect to the parameter β_2 is a symmetric function [$\sim \Omega^2 \exp(-\Omega^2/B^2)$], while the derivative of the phase with respect to the parameter β_3 is an antisymmetric function [$\sim \Omega^3 \exp(-\Omega^2/B^2)$]. Again, the spatial symmetry of the derivatives of the phase function determines the equivalence or nonequivalence of the coherent and single-photon multimode quantum states for calculating the elements of the QFIM.

Note that in this particular example, since $F_{12} = 0$ for both types of quantum states, the CR bound in Eq. (2) implies $\text{Var}(\theta_k) \leq 1/F_{kk}$ without any further assumptions or approximations.

Conclusions. – We have demonstrated that the most informative bound for the precision in the estimation of a set of parameters that characterize a phase object is the QCR. To derive this bound we have calculated the QFIM for two types of light waves, characterized by two corresponding quantum states; namely N copies of a single-photon multimode quantum state and a coherent multimode quantum state with mean photon number N . We have shown that the equivalence or nonequivalence of these quantum states for parameter estimation of phase objects through the computation of the QCR bound depends on the spatial symmetry of the phase introduced by the phase object.

The results presented in this work are a word of caution for experiments measuring the QFIM that make use of weak coherent states, while use single-photon quantum states in the corresponding theoretical analysis for the sake of simplicity.

ACKNOWLEDGMENTS

This work is part of the R&D project CEX2019-000910-S, funded by MCIN/AEI/10.13039/501100011033/. It is supported by Fundació Cellex, Fundació Mir-Puig, and Generalitat de Catalunya through the CERCA program. We acknowledge financial support from project QUISPAMOL (PID2020-112670GB-I00) funded by MCIN/AEI/10.13039/501100011033. This work is also part of the project 20FUN02 “POLight”, which has received funding from the EMPIR program co-financed by the Participating States and from the European Union’s Horizon 2020 research and innovation program. A.V. thanks the financial support from PREBIST that has received funding from the European Union’s Horizon 2020 research and innovation program under the Marie Skłodowska-Curie grant agreement No 754558.

Appendix A: Alternative derivation of Eq. (14) of the main text

The introduction of a spatially dependent phase $\{\varphi_k\}$ for each spatial coordinate (index k) is an unitary operation that can be represented by the operator

$$U = \exp \left[i \sum_k \varphi_k(\theta) a_k^\dagger a_k \right] \quad (\text{A1})$$

The output quantum state is thus

$$|\Phi(\theta)\rangle = U(\theta)|\alpha\rangle \quad (\text{A2})$$

The derivative of the quantum state with respect parameter θ_i is

$$|\Phi_i\rangle = \left(\frac{\partial U}{\partial \theta_i} \right) |\alpha\rangle = i \sum_k \left(\frac{\partial \varphi_k}{\partial \theta_i} \right) a_k^\dagger a_k |\alpha\rangle \quad (\text{A3})$$

so that

$$\langle \Phi | \Phi_i \rangle = i \sum_k \left(\frac{\partial \varphi_k}{\partial \theta_i} \right) \langle \alpha | a_k^\dagger a_k | \alpha \rangle \quad (\text{A4})$$

Similarly we can write

$$\begin{aligned} \langle \Phi_i | \Phi_j \rangle &= \sum_k \sum_{k'} \left(\frac{\partial \varphi_k}{\partial \theta_i} \right) \left(\frac{\partial \varphi_{k'}}{\partial \theta_j} \right) \langle \alpha | a_k^\dagger a_k a_{k'}^\dagger a_{k'} | \alpha \rangle \\ &= \sum_k \left(\frac{\partial \varphi_k}{\partial \theta_i} \right) \left(\frac{\partial \varphi_k}{\partial \theta_j} \right) \langle \alpha | a_k^\dagger a_k a_{k'}^\dagger a_{k'} | \alpha \rangle \\ &\quad + \sum_{k \neq k'} \left(\frac{\partial \varphi_k}{\partial \theta_i} \right) \left(\frac{\partial \varphi_{k'}}{\partial \theta_j} \right) \langle \alpha | a_k^\dagger a_k | \alpha \rangle \langle a_{k'}^\dagger a_{k'} | \alpha \rangle \end{aligned} \quad (\text{A5})$$

The elements of the QFIM are

$$\begin{aligned} F_{ij} &= 4 \langle \Phi_i | \Phi_j \rangle - 4 \langle \Phi | \Phi_i \rangle \langle \Phi | \Phi_j \rangle \\ &= 4 \sum_k \left(\frac{\partial \varphi_k}{\partial \theta_i} \right) \left(\frac{\partial \varphi_k}{\partial \theta_j} \right) \\ &\quad \times \left\{ \langle \alpha | a_k^\dagger a_k a_{k'}^\dagger a_{k'} | \alpha \rangle - \left[\langle \alpha | a_k^\dagger a_k | \alpha \rangle \right]^2 \right\} \\ &= \sum_k \left(\frac{\partial \varphi_k}{\partial \theta_i} \right) \left(\frac{\partial \varphi_k}{\partial \theta_j} \right) \langle (\Delta N_k)^2 \rangle \end{aligned} \quad (\text{A6})$$

where $N_k \equiv \langle a_k^\dagger a_k \rangle$ and the variance is $\langle (\Delta N_k)^2 \rangle = \langle N_k^2 \rangle - \langle N_k \rangle^2$. Making use of Eq. (A6) and that $\langle (\Delta N_k)^2 \rangle = |\alpha_k|^2$ for quantum coherent states, we obtain Eq. (13) on the main text.

Appendix B: Useful expressions to derive the QFIM elements and QCR bounds presented in the main text

Example I. – The spatial profile of the intensity of the illumination beam and the spatially-dependent phase are respectively given by Eqs. (16) and (17) in the main text. The derivatives of the phase φ with respect to the parameters sidewall angle α and height h are

$$\frac{\partial \varphi}{\partial \alpha} = -khx \operatorname{sech}^2 \alpha x \quad \frac{\partial \varphi}{\partial h} = k(1 - \tanh \alpha x). \quad (\text{B1})$$

Using $\theta_1 = \alpha$ and $\theta_2 = h$, from Eq. (4) we obtain

$$\langle \Phi | \Phi_1 \rangle = 0 \quad \langle \Phi | \Phi_2 \rangle = ik. \quad (\text{B2})$$

Similarly, from Eq. (5), we get

$$\begin{aligned} \langle \Phi_1 | \Phi_1 \rangle &= \left(\frac{2}{\pi}\right)^{1/2} \frac{\pi^2 - 6}{9} \frac{(kh)^2}{\sigma \alpha^3} \\ \langle \Phi_2 | \Phi_2 \rangle &= 2k^2 - \left(\frac{2}{\pi}\right)^{1/2} \frac{2k^2}{\sigma \alpha} \\ \langle \Phi_1 | \Phi_2 \rangle &= \left(\frac{2}{\pi}\right)^{1/2} \frac{k^2 h}{\sigma \alpha^2}. \end{aligned} \quad (\text{B3})$$

Example II. – The spectrum of the pulse as well as the frequency-dependent phase are respectively given by Eqs. (25) and (26) in the main text. The derivatives of the phase with respect to the parameters are

$$\frac{\partial \varphi}{\partial \beta_2} = \frac{1}{2} z \Omega^2 \quad \frac{\partial \varphi}{\partial \beta_3} = \frac{1}{6} z \Omega^3. \quad (\text{B4})$$

Using $\theta_1 = \beta_2$ and $\theta_2 = \beta_3$, similarly as above, we have

$$\langle \Phi | \Phi_1 \rangle = \frac{z B^2}{4} \quad \langle \Phi | \Phi_2 \rangle = 0, \quad (\text{B5})$$

and from Eq. (5)

$$\begin{aligned} \langle \Phi_1 | \Phi_1 \rangle &= \frac{3z B^4}{16} \\ \langle \Phi_2 | \Phi_2 \rangle &= \frac{5z B^6}{96} \\ \langle \Phi_1 | \Phi_2 \rangle &= 0. \end{aligned} \quad (\text{B6})$$

[1] D. Murphy and M. Davidson, *Fundamentals of Light Microscopy and Electronic Imaging*, Fundamentals of Light Microscopy and Electronic Imaging (Wiley, 2012).

[2] D. C. Flanders, Submicrometer periodicity gratings as artificial anisotropic dielectrics, *Applied Physics Letters* **42**, 492 (1983).

[3] L. Cissoto, S. F. Pereira, and H. P. Urbach, Analytical calculation on the determination of steep side wall angles from far field measurements, *Journal of Optics* **240**, 065601 (2018).

[4] A. S. Holevo, *Probabilistic and statistical aspects of quantum theory*, Vol. 1 (Springer Science & Business Media, 2011).

[5] P. R. Bevington and D. K. Robinson, *Data reduction and error analysis for the physical sciences* (Mc Graw Hill, 1980).

[6] C. W. Helstrom, Estimation of object parameters by a quantum-limited optical system, *JOSA* **60**, 233 (1970).

[7] M. Tsang, R. Nair, and X.-M. Lu, Quantum theory of superresolution for two incoherent optical point sources, *Physical Review X* **6**, 031033 (2016).

[8] M. Paúr, B. Stoklasa, Z. Hradil, L. L. Sánchez-Soto, and J. Rehacek, Achieving the ultimate optical resolution, *Optica* **3**, 1144 (2016).

[9] C. Napoli, S. Piano, R. Leach, G. Adesso, and T. Tufarelli, Towards superresolution surface metrology: Quantum estimation of angular and axial separations, *Physical Review Letters* **122**, 140505 (2019).

[10] L. Pezze, A. Smerzi, M. K. Oberthaler, R. Schmied, and P. Treutlein, Quantum metrology with nonclassical states of atomic ensembles, *Review of Modern Physics* **90**, 035005 (2018).

[11] S. Zhou and L. Jiang, Modern description of rayleigh's criterion, *Physical Review A* **99**, 013808 (2019).

[12] A. Fujiwara, One-parameter pure state estimation based on the symmetric logarithmic derivative, *Math. Eng. Tech. Rep* **94** (1994).

[13] K. Matsumoto, A geometrical approach to quantum estimation theory, in *Asymptotic Theory Of Quantum Statistical Inference: Selected Papers* (World Scientific, 2005) pp. 305–350.

[14] K. Matsumoto, A new approach to the cramér-rao-type bound of the pure-state model, *Journal of Physics A: Mathematical and General* **35**, 3111 (2002).

[15] A. Fujiwara, Multi-parameter pure state estimation based on the right logarithmic derivative, *Math. Eng. Tech. Rep* **94**, 94 (1994).

[16] A. Fujiwara and H. Nagaoka, Quantum fisher metric and estimation for pure state models, *Physics Letters A* **201**, 119 (1995).

[17] L. Pezzè, M. A. Ciampini, N. Spagnolo, P. C. Humphreys, A. Datta, I. A. Walmsley, M. Barbieri, F. Sciarrino, and A. Smerzi, Optimal measurements for simultaneous quantum estimation of multiple phases, *Physical Review Letters* **119**, 130504 (2017).

[18] D. Safranek, Simple expression for the quantum information matrix, *Physical Review A* **97**, 042322 (2018).

[19] S. Z. Ang, R. Nair, and M. Tsang, Quantum limit for two-dimensional resolution of two incoherent optical point sources, *Physical Review A* **95**, 063847 (2017).

- [20] Y. Zhou, J. Yang, J. D. Hassett, S. M. H. Rafsanjani, M. Mirhosseini, A. N. Vamivakas, A. N. Jordan, Z. Shi, and R. W. Boyd, Quantum-limited estimation of the axial separation of two incoherent point sources, *Optica* **6**, 534 (2019).
- [21] J. Hassett, T. Malhorta, M. Alonso, R. Boyd, S. H. Rafsanjani, and A. Vamivakas, Sub-rayleigh limit localization with a spatial mode analyzer, in *Laser Science* (Optical Society of America, 2018) pp. JW4A-124.
- [22] M. Jarzyna and R. Demkowicz-Dobrzanski, Quantum interferometry with and without an external phase reference, *Physical Review A* **85**, 011801(R) (2012).
- [23] S. M. Barnett and P. M. Radmore, *Methods in theoretical quantum optics*, Oxford series in optical and imaging sciences (Clarendon Press - Oxford, 2002).
- [24] J. P. Torres and L. J. Salazar-Serrano, Weak value amplification: a view from quantum estimation theory that highlights what it is and what isn't, *Scientific reports* **6**, 1 (2016).
- [25] S. Soman, S. F. Pereira, and O. E. Gwahary, Diffraction grating parameter retrieval using non-paraxial structured beams in coherent fourier scatterometry, *Journal of Optics* **24**, 034006 (2022).
- [26] L. Cisotto and P. H. Urbach, Amplitude and phase beam shaping for highest sensitivity in sidewall angle detection, *JOSA A* **34**, 52 (2017).
- [27] J. E. Prussing, The principal minor test for semidefinite matrices, *Engineering notes* **9**, 121 (1986).